JOURNAL OF GEOPHYSICAL RESEARCH VOL. 68, NO. 13 JULY 1, 1963

Synchrotron Radiation Calculations for the Artificial Radiation Belt

M. P. NAKADA

NASA Goddard Space Flight Center, Greenbelt, Maryland

Abstract. Synchrotron radiation from the artificial radiation belt is calculated in some detail. The angular distribution of the electrons and of the synchrotron radiation is considered. Omnidirectional electron fluxes due to Van Allen, Frank, and O'Brien and Brown and Gabbe are used to derive directional fluxes. Temperatures as a function of frequency and of the geomagnetic latitude at 30 Mc/s are calculated. Results are compared with measurements.

Introduction. In a recent issue of this journal *Peterson and Hower* [1963] discussed synchrotron radiation from the artificial radiation belt and presented calculations for sky temperatures that might be expected at the geomagnetic equator according to electron flux estimates by *Hess* [1963]. In the same issue, different flux estimates by *Brown and Gabbe* [1963] (BG) and *Van Allen, Frank, and O'Brien* [1963] (VFO) were reported. Synchrotron radiation calculations for the BG and VFO electron fluxes have been made with the inclusion of the angular distributions of the electrons and the synchrotron radiation. The dipole geomagnetic field has been assumed, and geomagnetic latitudes have been used. The fission product electron spectrum due to *Carter et al.* [1959] has been assumed.

Angular distribution of electrons. Figure 1 shows the electron flux maps due to BG and VFO. The dotted parts of the VFO map are extrapolations by the present author. Figure 2 shows his view of equatorial fluxes for BG and VFO; the marked points were taken from those authors.

Given these omnidirectional fluxes, the directional fluxes have been obtained following *Ray* [1960] and *Farley and Sanders* [1962]. The omnidirectional flux J along a magnetic field line is plotted as a function of the magnetic field strength. Because of the scarcity of experimental points, analytic forms of J were used to fit the plotted points. Figure 3 compares J values taken from Figures 1 and 2 with J values used in the calculations. The analytic form used for BG is proportional to $(B - B_{max})^2$, and that for VFO is proportional to $(B - B_{max})$, where B is the magnetic field for J and B_{max} is the field where J becomes small. The equatorial omnidirectional flux, J_0, and B_{max} are then sufficient to determine J along a field line. Equation 6 from

(NASA RP-67)

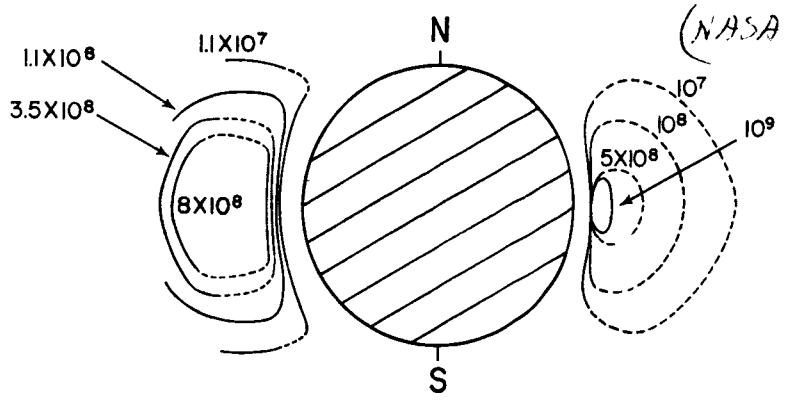

Fig. 1. The BG and VFO flux maps used in the calculations. Numbers are omnidirectional fluxes in electrons per centimeter² second.

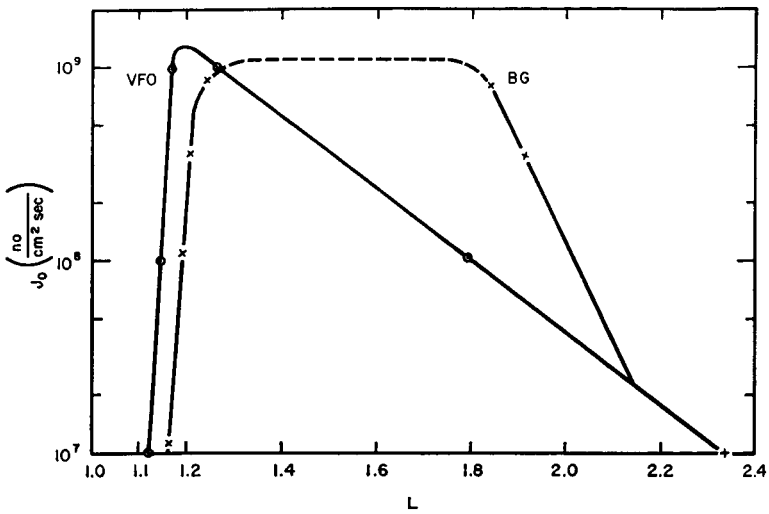

Fig. 2. Omnidirectional fluxes along the geomagnetic equator.

Farley and Sanders [1962] has been used to determine the equatorial directional flux from the omnidirectional flux. Liouville's theorem and the equation of motion of the electrons, $\sin^2\theta = (B/B_0)\sin^2\theta_0$, have been used to give directional fluxes away from the equator. θ and B are pitch angles and magnetic fields; the subscript zero refers to equatorial values. Figure 4 shows shapes of equatorial directional fluxes as a function of pitch angle.

For later comparison with the width of synchrotron radiation, the half-angle of electron angular distributions at the equator has been plotted in Figure 5. The half-angle is the pitch angle measured from the normal to the field line to where the directional flux is one-half of the direction flux at 90° to the field. Figure 6 shows variations in equatorial angles with geomagnetic latitude.

Angular distribution of synchrotron radiation. The power radiated in the nth harmonic of the cyclotron frequency into a unit solid angle at angle ψ with the instantaneous orbital plane has been given by *Schwinger* [1949]. The ψ-dependent part is given by

$$[J_n'(n\beta\cos\psi)]^2 + [(\tan^2\psi)/\beta^2] \cdot [J_n(n\beta\cos\psi)]^2$$

where J_n' and J_n are Bessel functions and β is the ratio of the velocity of the electron to the velocity of light. The angular distribution relative to $\psi = 0$ has been evaluated. Angles at which the power radiated is one-half of the $\psi = 0$ values are plotted in Figure 7 for a number of electron energies. The abscissa is $n/(1-\beta^2)^{1/2}$, which is equal to $\nu/(2.8B\sin\theta)$, where ν is the frequency in megacycles per second, B is the magnetic field in gauss, and θ is the pitch angle of the electron relative to B. These results show a rather small dependence of the angular distribution on electron energy for a given $\nu/(B\sin\theta)$. At 30 Mc/s for $B = 0.2$ gauss, a value that is near the earth, $\psi_{1/2}$ is about 7.8°. At 50 Mc/s for the same B, $\psi_{1/2}$ is about 6.0°. For smaller $B\sin\theta$, $\psi_{1/2}$ is, of course, narrower.

Thus, the angular distribution of the synchrotron radiation is usually narrower than that of the electron angular distribution for frequencies and magnetic fields of interest in this report.

Calculation of temperatures. The brightness along a line of sight is given by

$$\int \frac{dP}{d\Omega}\, dR$$

where $dP/d\Omega$ is the power emitted per unit volume along the line of sight per steradian. The integration is along the line of sight. Since the synchrotron radiation pattern is usually narrower than that of the electrons, the following approximation has been used for the brightness b:

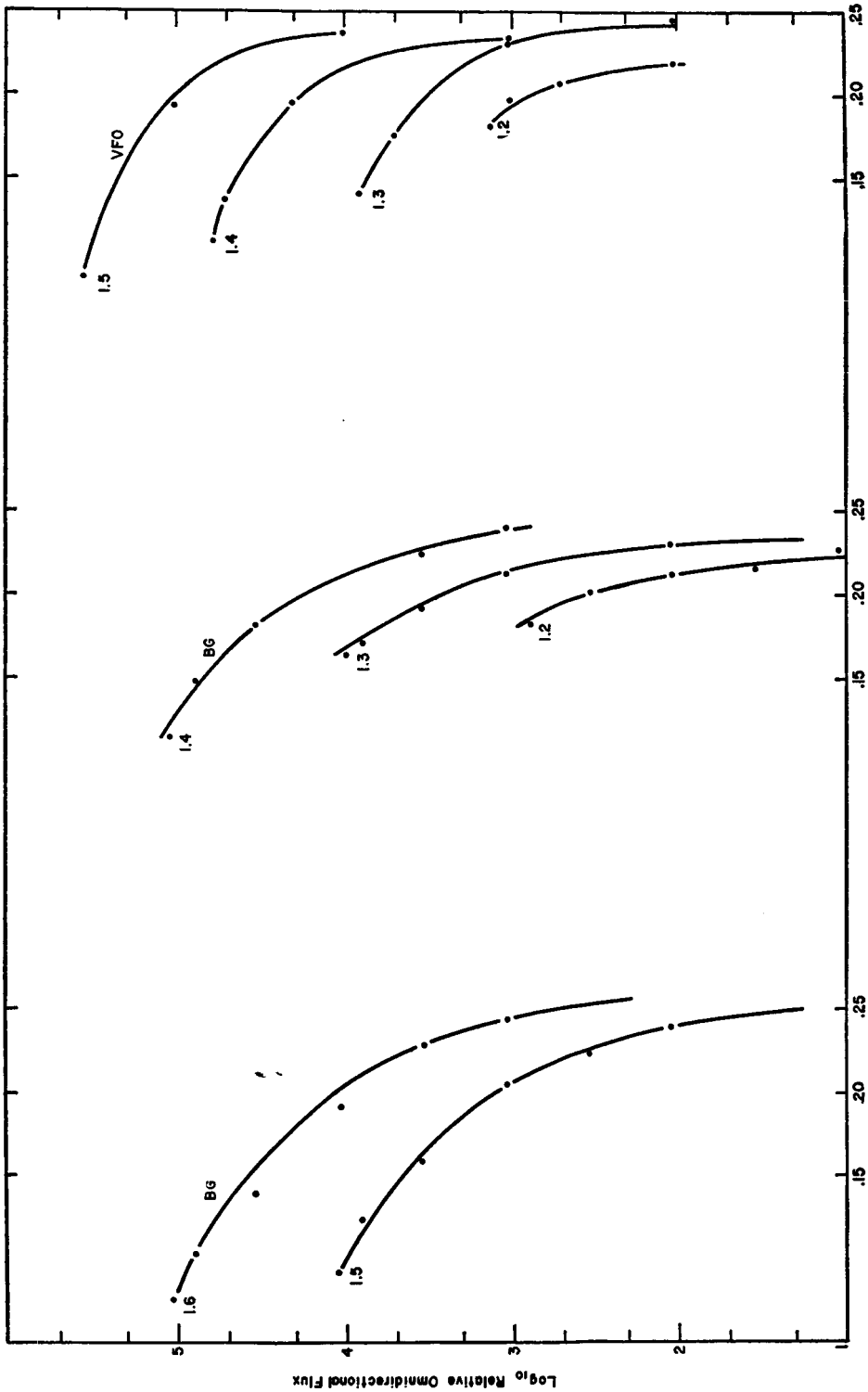

Fig. 3. Comparison of relative omnidirectional fluxes versus B along a magnetic field line. Dots are experimental values. Lines are the assumed analytic forms used in the calculations.

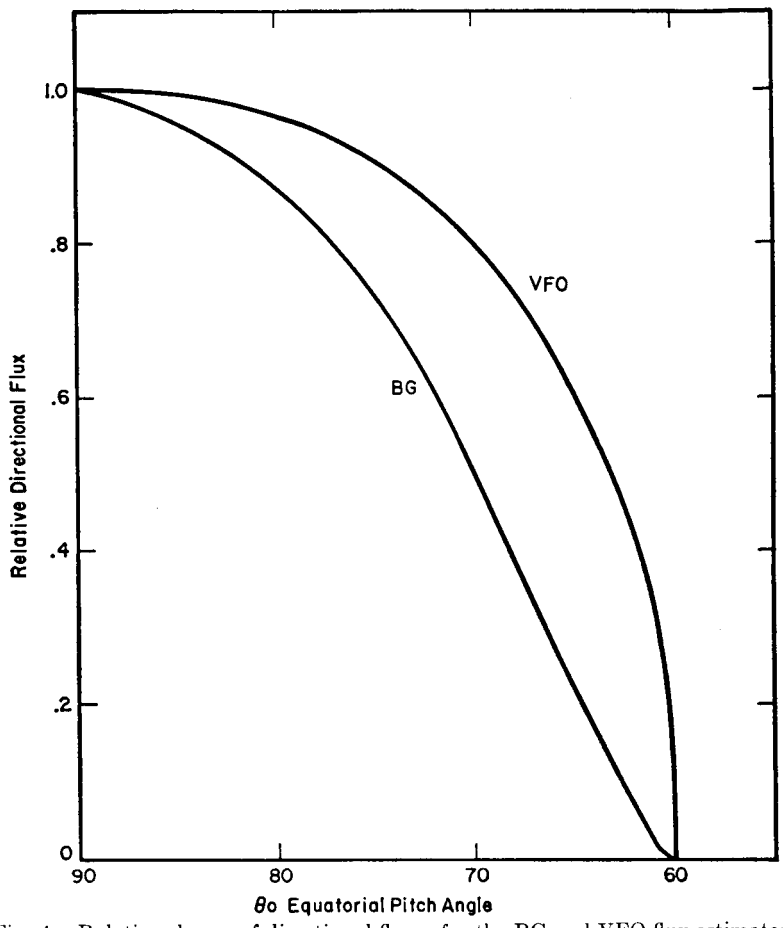

Fig. 4. Relative shapes of directional fluxes for the BG and VFO flux estimates.

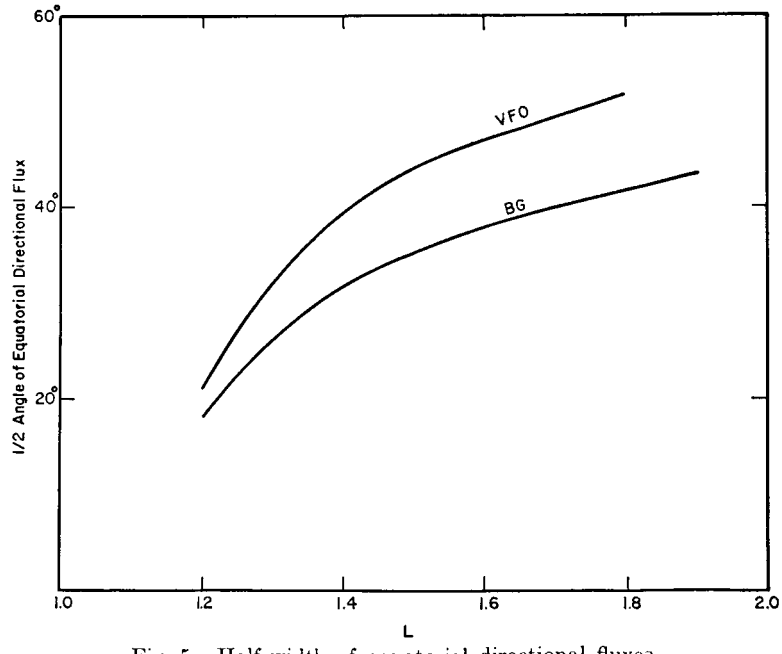

Fig. 5. Half-width of equatorial directional fluxes.

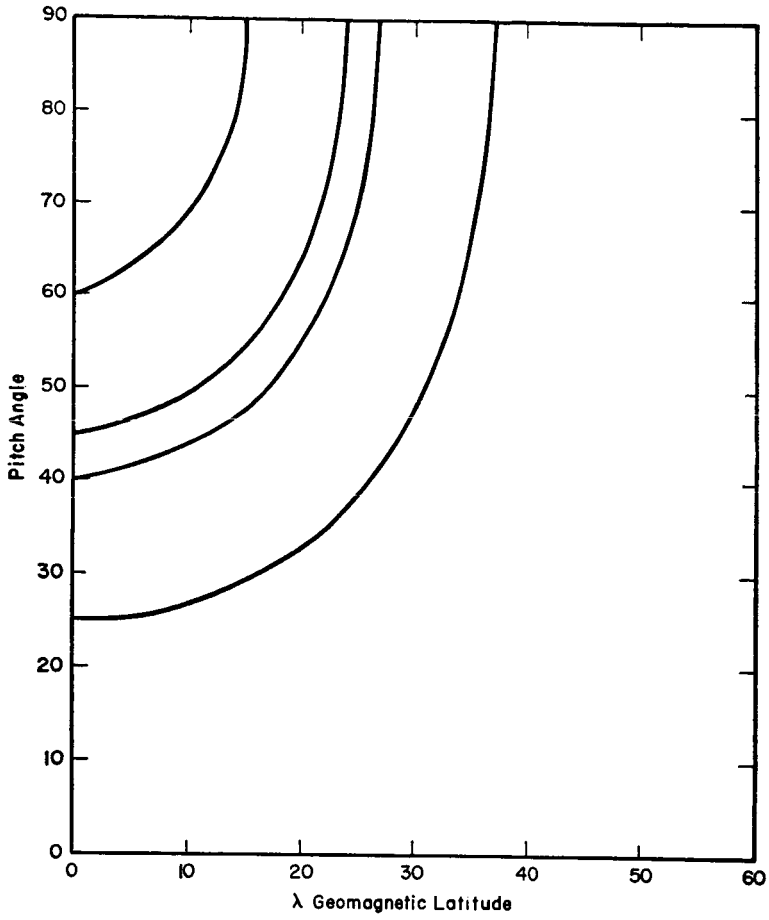

Fig. 6. Variation of pitch angle with geomagnetic latitude.

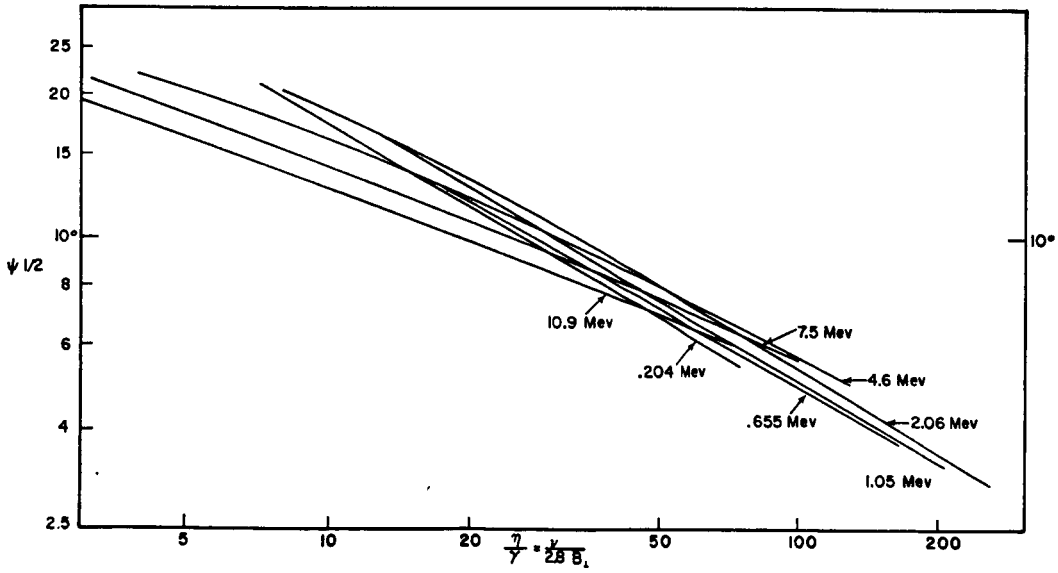

Fig. 7. Half-width of the synchrotron radiation pattern. The abscissa is $\nu/(2.8B \sin \theta)$, where ν is the frequency in megacycles per second, B is the magnetic field in gauss, and θ is the pitch angle of an electron.

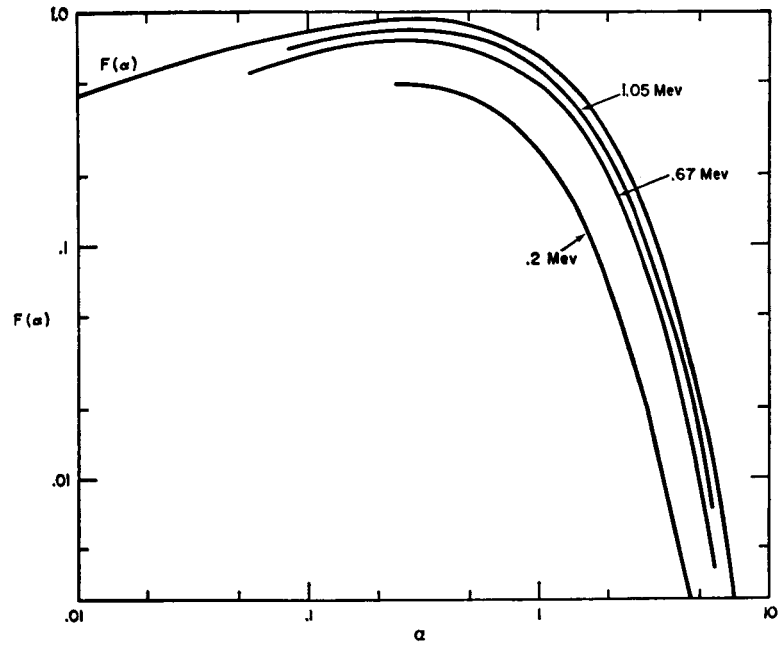

Fig. 8. Comparison between relativistic and nonrelativistic synchrotron radiation-power formula.

$$b(\nu) = \int P(\nu, B \sin \theta) \frac{j(\theta)}{\beta c} \, dR \qquad (1)$$

$P(\nu, B \sin \theta)$ is the total power emitted per unit frequency at frequency ν for an electron moving toward the observer. This electron has a pitch angle θ with the magnetic field B. $j(\theta)$ is the directional flux of fission product decay electrons. $P(\nu, B \sin \theta)$ is given by

$$P(\nu, B \sin \theta) = \int P(E, \nu/[B \sin \theta]) N(E) \, dE$$

where E is the electron energy, $N(E)$ is the normalized electron spectrum, and $P(E, \nu/B \sin \theta)$ is the total power emitted per unit frequency at ν and $B \sin \theta$ for an electron with energy E.

Although equation 1 is an approximation, errors introduced through its use are small for electron and radiation pattern widths considered in this report. To obtain an exact $dP/d\Omega$, the radiation pattern (slightly different at each angle and electron energy) should be folded into the electron angular distribution, and the result of this fold along the line of sight should be used. If the electron and radiation distributions are assumed to be Gaussian, the result of the fold will give a pattern whose width is given by the square root of the sum of the squares of the assumed Gaussians. For most distributions considered in this report, the resulting Gaussian is only a few per cent broader than an appropriate electron distribution Gaussian. Since both the electron and radiation distributions fall off more rapidly than appropriate Gaussians, the true fold should be narrower than the result of folding the Gaussians. To assess the effect of folded patterns that are broader than the electron pattern, calculations have been made by increasing the electron width to exceed the result of the fold at all points. The calculated temperatures indicate that errors introduced through the use of equation 1 are small.

The relativistic formula for $P(\nu, B \sin \theta, E)$ has been used [*Westfold*, 1959]

$$P(\nu, B \sin \theta, E) = CB \sin \theta \alpha \int_{\alpha}^{\infty} K_{5/3}(\eta) \, d\eta \qquad (2)$$

C is a constant equal to 2.34×10^{-22} erg/sec cycle/sec,

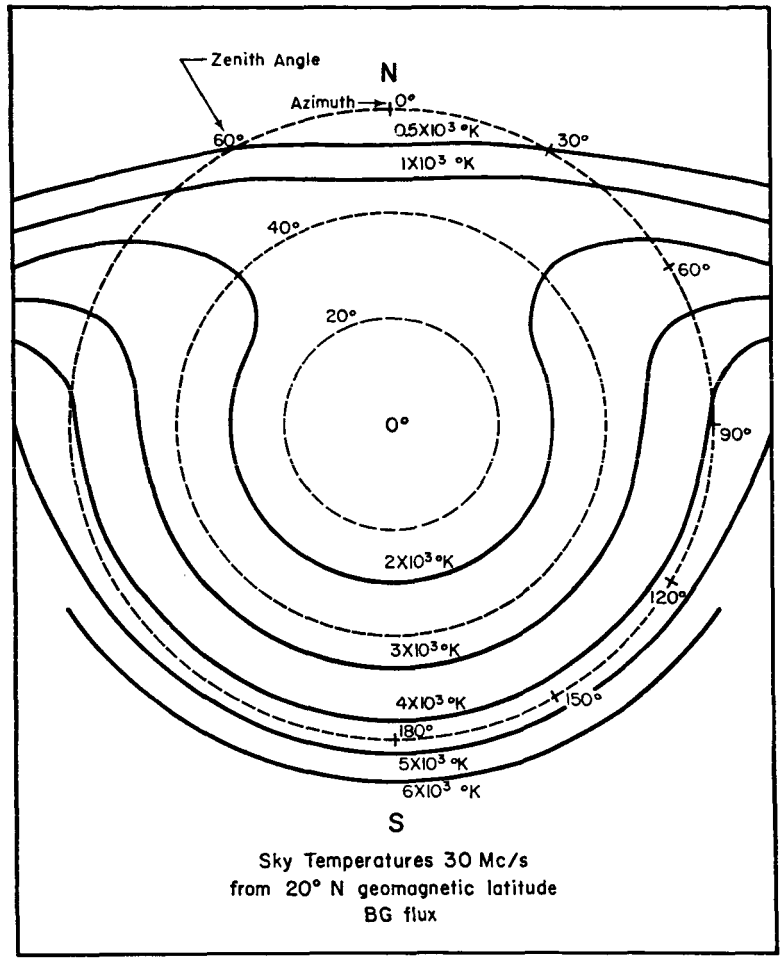

Fig. 9. Sky brightness map due to the artificial radiation belt. Solid lines are isophotos.

$$\alpha = \frac{\nu(\mathrm{Mc/s})}{4.2\gamma^2 B \sin\theta}$$

$$\gamma = (1 - \beta^2)^{-1/2}$$

and $K_{5/3}$ is a Bessel function. This formula gives upper limit values.

$$\alpha \int_{\alpha}^{\infty} K_{5/3}(\eta)\, d\eta$$

is plotted in Figure 8. Corresponding values for the nonrelativistic formula [*Schwinger*, 1949, formula III.28] are also shown in Figure 8. These results indicate that, where radiation by electrons is efficient, the relativistic formula is a satisfactory though upper-limit approximation.

Equation 1 with $\beta = 1$ has been used to evaluate sky brightness. The Rayleigh-Jeans approximation to the Planck radiation formula has been used to convert brightness to temperatures, T; $b = 2kT/\lambda^2$, where k is Boltzmann's constant and λ is the wavelength.

Figure 9 shows sky temperatures at 30 Mc/s for the BG flux for an observer at 20°N geomagnetic latitude.

Figure 10 shows temperatures as a function of frequency for the BG and VFO fluxes for an observer at the geomagnetic equator looking vertically. At the geomagnetic equator, the temperatures calculated for a narrow-beam antenna and a $\cos^2 Z$ antenna are very nearly the same. Z is the zenith angle.

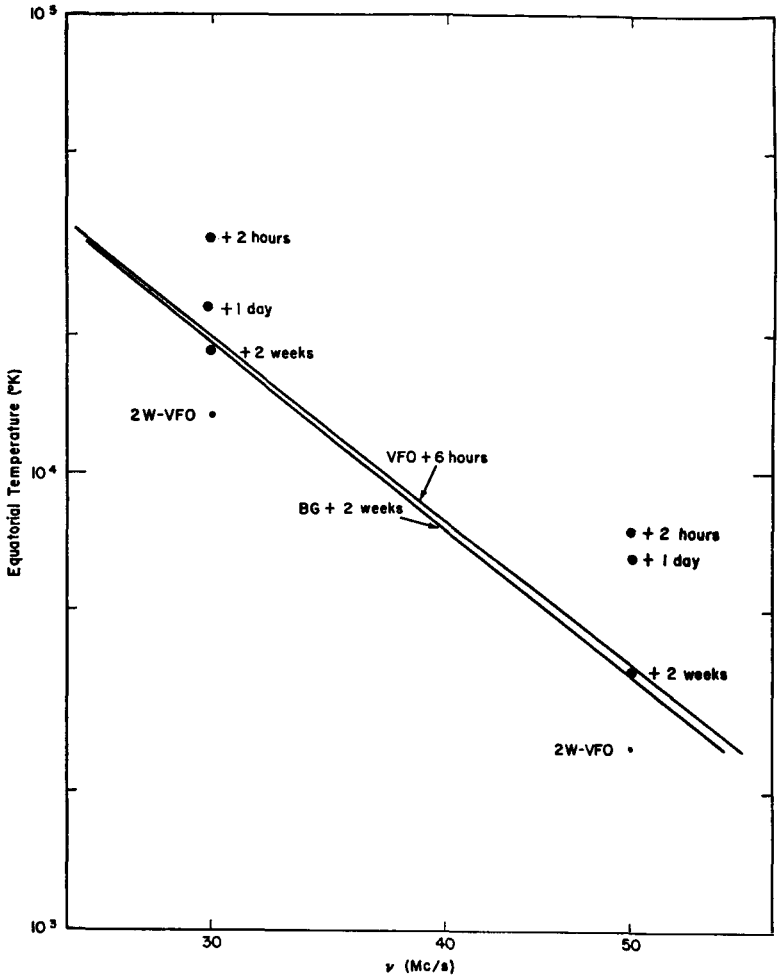

Fig. 10. Comparison between calculated and observed sky temperatures at the geomagnetic equator.

Despite the time difference for the two flux estimates (VFO at 6 hours and BG at 2 weeks after the detonation), the results are very nearly the same. The VFO values tend to be higher at higher frequencies. This is to be expected, since VFO fluxes are higher at lower altitudes and higher frequencies show a greater decrease in radiation with altitude [*Peterson and Hower*, 1963].

Experimental points are taken from measurements of *Ochs et al.* [1963] with times after shot adjacent. Their 0600 local time background temperature at 50 Mc/s of 5200°K was obtained from their sky survey [*Ochs et al.*, 1963]. The 30-Mc/s background temperature of 15,000°K at 0600 local time was obtained from their ratio of 30-Mc/s to 50-Mc/s temperatures before the shot.

Temperatures have also been calculated at 30 and 50 Mc/s for an estimated flux for VFO at 2 weeks after the shot. The BG equatorial flux has been used from $L = 1.16$ to $L = 1.28$; the VFO flux has been used from $L = 1.28$ to $L = 2.3$. The BG angular distribution has been used. Temperatures for this flux estimate are labeled 2W-VFO and are also plotted in Figure 10.

The calculated changes in temperatures with geomagnetic latitude at 30 Mc/s for observers looking vertically with $\cos^2 Z$ antennas are plotted in Figures 11 and 12 for the BG and VFO flux estimates. The experimental measurements from *Dyce and Horowitz* [1963] are

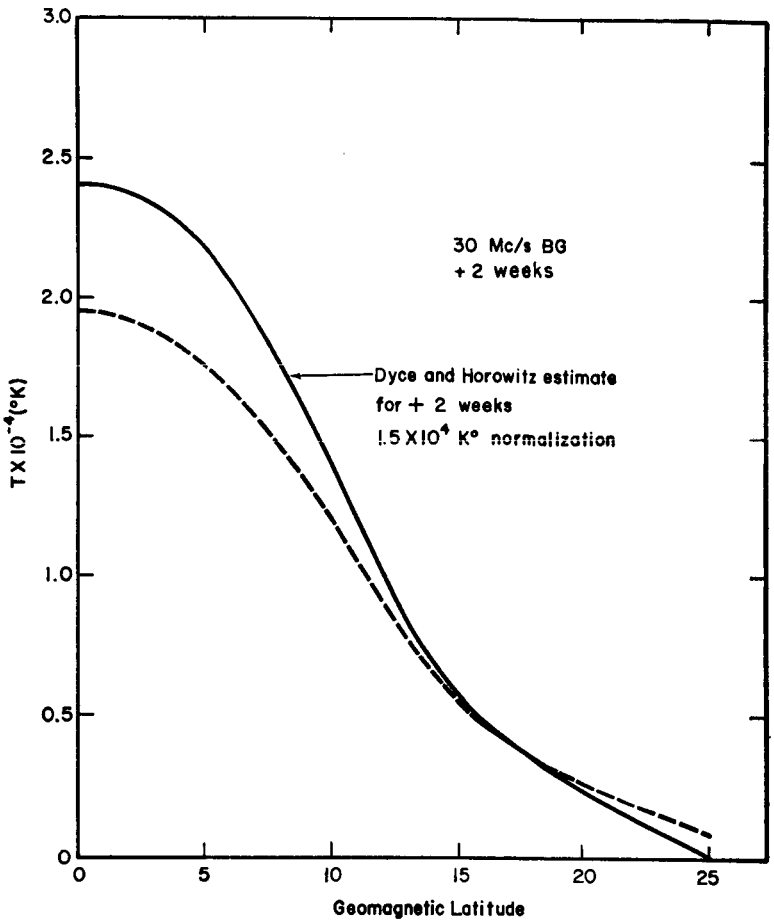

Fig. 11. Dotted line shows predicted sky temperatures for vertically directed antennas with $\cos^3 Z$ pattern for the BG flux estimates at +2 weeks at different geomagnetic latitudes. Solid curve is the experimental curve of Dyce and Horowitz; this curve has been renormalized, and a decay has been included.

temperatures normalized to preshot diurnal minimum for an approximately $\cos^3 Z$ antenna. *Dyce and Horowitz* [1963] used 10^4 deg K for this minimum temperature. This seems rather low for their antennas, since interpolation of *Turtle et al.*'s [1963] results at 26.3 and 38 Mc/s gives a minimum temperature of 10^4 deg K at 30 Mc/s for a 15° right ascension by 44° declination antenna. Estimates for a $\cos^3 Z$ antenna, using the absolute temperature maps due to *Turtle et al.* [1963] and *Steiger and Warwick* [1961], indicate that the normalization temperature at 30 Mc/s for the diurnal minimum was probably near 1.5×10^4 deg K. A latitude distribution using this estimated normalization temperature is plotted in Figures 11 and 12. For the BG comparison, a $(1 + t/T)^{-1}$ decay with $T =$ 60 days has been used at all latitudes, although +2 week measurements at the geomagnetic equator are in agreement with calculated temperatures (see Figure 10).

Discussion. The results of calculated equatorial temperatures seem to indicate that the VFO flux may be inadequate to explain measured temperatures at +6 hours. The BG flux appears to give satisfactory agreement with observations at 2 weeks.

The latitude distribution is more sensitive to fluxes at larger L values. The VFO flux shows greater temperature deviations from observa-

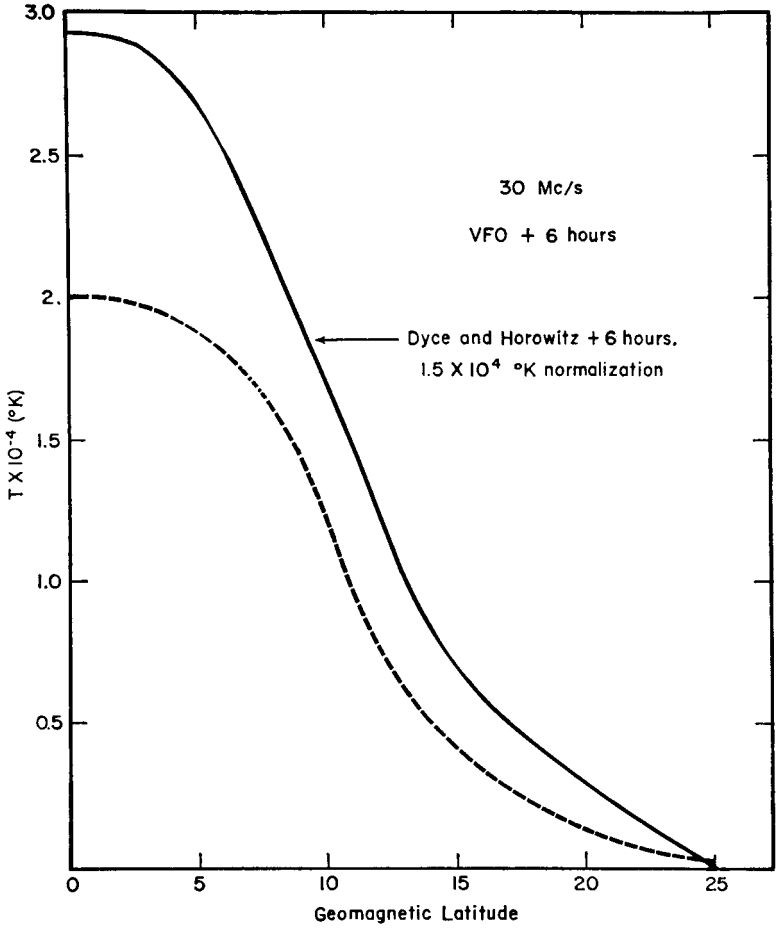

Fig. 12. Dotted line shows predicted sky temperatures at +6 hours for vertically directed antennas with $\cos^3 Z$ pattern for the VFO flux estimate at different geomagnetic latitudes. Solid curve is the renormalized experimental curve of Dyce and Horowitz.

tions at higher latitudes. Whether the BG flux estimate is in agreement with observations will depend on measurements of absolute temperatures for the antennas that were used and on measurements at +2 weeks.

The largest difference between the two flux estimates is for L values greater than 1.28. If a fission spectrum is assumed for the difference between the two flux estimates ($L > 1.28$), the calculated equatorial temperature for this difference flux at 50 Mc/s is 941°K. The BG angular distribution has been used in this calculation, which is for a narrow-beam antenna pointed vertically. This temperature may be compared with the minimum detectable temperature of about 40°K at 50 Mc/s [*Ochs et al.*, 1963] using polarization techniques. *Ochs et al.* [1963] attempted to observe synchrotron radiation from the natural radiation belt immediately before the detonation but detected no positive signal. From this it may be inferred that, if the difference between the two flux estimates was natural, but had a spectrum similar to that of fission product decay electrons, it should have been detectable. Electrons with energy less than 2 Mev do not contribute appreciably to 50-Mc/s radiation for this difference flux.

BG are unable to distinguish any spectral difference between regions where the fission spectrum was highly probable and the difference-flux regions. However, their detector is not sensitive enough to distinguish between spec-

trums in which the greater-than-2-Mev parts may be very different.

VFO find from their Injun 1 data that the artificial belt spectrum is considerably 'harder' than the natural one at L of about 4, but whether this hardening extends to equatorial regions in the same way is not known.

Although Explorer 12 traversed this region and had a detector sensitive to electrons with energy greater than 1.6 Mev, detailed studies have not been published. Perhaps a study of Explorer 12 results and spectral and decay studies of Explorer 14 and 15 and Telstar results in conjunction with the negative polarization results of synchrotron radiation before the shot will shed light on what fraction of the BG observations was natural.

Conclusions. Angular distributions of electrons have been used that are consistent with published omnidirectional flux maps of BG and VFO.

The angular distribution of synchrotron radiation has been found to be considerably narrower than that of electrons for most situations. The fold of the synchrotron radiation pattern onto the electron angular distribution should be slightly wider than the electron pattern.

Since the electron distribution has been used to represent the result of the folded radiation and electron distribution, calculations have been made with electron distributions that were broader than the result of the fold at all locations. The deviations due to this broadening were found to be small.

Although the relativistic radiation formula tends to give upper-limit results, evaluation of the nonrelativistic formula shows that the relativistic approximation is quite adequate even at frequencies lower than those considered here.

For the assumed magnetic field, electron spectrum, and fluxes, these calculations have been estimated to have an uncertainty of about 10 per cent.

The VFO flux estimate has been found inadequate to explain observed temperature at the equator and at higher latitudes.

Conclusions about the adequacy of the BG estimate will depend on absolute calibration of antennas and on later results, although present estimates of absolute temperatures for the antennas indicate good agreement between measured and calculated temperatures.

Calculated temperatures for the difference between the BG and VFO fluxes for L greater than 1.28 set limits on electron spectrums in the natural radiation belt before the shot. This result, in conjunction with satellite measurements, may determine what fraction of the BG flux estimate was natural.

Acknowledgments. I gratefully acknowledge the work of Tom Michels, who made the calculations involving Bessel functions. Robert Baxter set up the code for the detailed temperature calculation; his work is gratefully acknowledged.

References

Brown, W. L., and J. D. Gabbe, The electron distribution in the earth's radiation belts during July 1962 as measured by Telstar, *J. Geophys. Res., 68,* 607–618, 1963.

Carter, R. E., F. Reines, J. J. Wagner, and M. E. Wyman, Free antineutrino absorption cross section, 2, Expected cross section from measurements of fission fragment electron spectrum, *Phys. Rev., 113,* 280, 1959.

Dyce, R. B., and S. Horowitz, Measurement of synchrotron radiation at central Pacific sites, *J. Geophys. Res., 68,* 713–721, 1963.

Farley, T. A., and N. L. Sanders, Pitch angle distributions and mirror point densities in the outer radiation zone, *J. Geophys. Res., 67,* 2159–2168, 1962.

Hess, W. N., The artificial radiation belt made on July 9, 1962, *J. Geophys. Res., 68,* 667–683, 1963.

Ochs, G. R., D. T. Farley, Jr., K. L. Bowles, and P. Bandyopadhay, Observations of synchrotron radio noise at the magnetic equator following the high-altitude nuclear explosion of July 9, 1962, *J. Geophys. Res., 68,* 701–711, 1963.

Peterson, A. M., and G. L. Hower, Synchrotron radiation from high-energy electrons, *J. Geophys. Res., 68,* 723–734, 1963.

Ray, E. C., On the theory of protons trapped in the earth's magnetic field, *J. Geophys. Res., 65,* 1125–1134, 1960.

Schwinger, J., On the classical radiation of accelerated electrons, *Phys. Rev., 75,* 1912, 1949.

Steiger, W. R., and J. W. Warwick, Observations of cosmic radio noise at 18 Mc/s in Hawaii, *J. Geophys. Res., 66,* 57–66, 1961.

Turtle, A. J., J. F. Pugh, S. Kenderdine, and I. I. K. Pauliny-Toth, The spectrum of the galactic radio emission, 1, Observations of low resolving power, *Monthly Notices Roy. Astron. Soc., 124,* 297, 1962.

Van Allen, J. A., L. A. Frank, and B. J. O'Brien, Satellite observations of the artificial radiation belt of July 1962, *J. Geophys. Res., 68,* 619–627, 1963.

Westfold, K. C., The polarization of synchrotron radiation, *Astrophys. J., 130,* 241, 1959.

(Manuscript received April 10, 1963.)